Supporting Information: Optical Properties of Metal-Ion-Mediated Au_{25} Nanocluster-Based Assemblies

Hanna Jääskö [1], Sami Malola[1], and Hannu Häkkinen[1,2*]

[1]Department of Physics, Nanoscience Center, University of Jyväskylä, Jyväskylä 40014, Finland
[2]Department of Chemistry, Nanoscience Center, University of Jyväskylä, Jyväskylä 40014, Finland

Contents

List of Figures

1 Structural modifications and magnetic state

The four-cluster assemblies, named as Au_{25}-Mg, Au_{25}-Co, Au_{25}-Ni and Au_{25}-Cu, were originally taken from the crystal structures published by Kim et al.[1], where the following modifications were made. First, four clusters coordinated by the same metal ion were extracted, see Figure S1. Then, all other coordinating metal ions and water molecules were removed from the model, and all *p*-MBA ligands not involved in the coordination bonds were protonated.

Moreover, one $[Au_{25}(p\text{-MBA})_{18}]^-$ cluster was taken from each crystal structure, and all *p*-MBA ligands were protonated. Lastly, the metal ion/ions coordinated to four *p*-MBA ligands were extracted as smaller coordination complexes in which the free sulfur atoms were saturated by protons. The modifications to the structures were performed with the Mercury software[2]. In total, the calculations were performed for three different kinds of systems: 1) the four-cluster assembly, 2) $[Au_{25}(p\text{-MBA})_{18}]^-$ cluster, and 3) coordination complex.

The electron configuration of Ni^{2+} is $[Ar]3d^8$, therefore the magnetic moment for both Ni atoms was set to +2. Au_{25}-Ni converged to a ferromagnetic ground state. The electron configuration of Co^{2+} is $[Ar]3d^7$, so the magnetic moment was set to +3 per Co atom. Whether the ground state of Au_{25}-Co is antiferromagnetic or ferromagnetic cannot be definitely concluded. It is known that the magnetic exchange between two Co^{2+} tends to be antiferromagnetic. In a Co-O-Co bridge, where O is from H_2O, the distance and angle of the bridge can affect whether they are in an antiferromagnetic state or a weakly ferromagnetic state[3,4]. Au_{25}-Co converged to a ground state where both magnetic moments point in the same direction, but they are not equal. This explains the low energy signal in the spectra, since the other spin channel had partially filled Kohn-Sham orbitals.

2 Computational details

We employed the grid-based projector-augmented wave (GPAW)[5] code for all the density functional theory (DFT) calculations. We used the Gritsenko–van Leeuwen–van Lenthe–Baerends–solid-correlation (GLLB-SC) functional[6] for the ground state calculations and the Perdew-Burke-Ernzerhof (PBE) functional[7] as the exchange-correlation kernel for the LR-TDDFT calculation that was used to calculate the optical absorption and circular dichroism (CD) spectra. GLLB-SC has been successful in estimating the band gaps for semiconductor-like materials by accounting the discontinuity derivative, which widens the gap. For Au_{25}-Mg

the ground-state calculation was done as spin-paired and for Au_{25}-Co, Au_{25}-Ni and Au_{25}-Cu as spin-polarized, see the previous section discussion about magnetic moments. For all calculations we used real-space grids with 0.25Å grid spacing and 6Å vacuum around the system. The Kohn-Sham orbitals are visualized with VMD[8]. The total charge of the cluster assemblies was set to $-4|e|$ originating from the four $[Au_{25}(p\text{-MBA})_{18}]^-$ clusters.

For Au_{25}-Co, we had to slightly finetune the convergence criteria from the default values. By default, the self-consistent field (SCF) cycle of ground state calculation is considered to be converged if energy changes less than 0.5 meV per valence electron (last three iterations), density changes less than 0.0001 electrons per valence electron and the integrated value of the square of the residuals of the Kohn-Sham equations is less than $4 \cdot 10^{-8}$ eV^2 per valence electron. For this calculation, the criteria for the Kohn-Sham equations and density were loosened to $1 \cdot 10^{-6}$ and 0.0008, respectively. The choice of the criteria is validated by the absorption spectrum of Au_{25}-Co which is consistent with the spectra of the other systems, as well as with the spectrum of individual $Au_{25}(p\text{-MBA})_{18}$ cluster taken from the Co assembly. Moreover, the calculated optical gap follows the trend observed in the other assemblies and agrees well with the experimental optical gap reported in[1].

Due to the computational cost of spin-polarized calculations for larger systems, we used an energy cut-off of 2.5 eV for the LR-TDDFT calculations. In order to systematically compare the absorption spectra, we used the same cut-off for the spin paired calculation. For all systems, the optical band gap was found well below 2 eV, and the spectra were confirmed to be converged at the optical band gap region, as can be seen in Figure S2. The oscillator and rotatory strengths of the transitions were smoothed by 0.1 eV Gaussians to obtain the final spectra.

To understand the origins of the peaks in the absorption spectra, we performed the transition contribution map (TCM) analysis that is based on the time-dependent density functional perturbation theory (TD-DFPT)[9,10]. TCM analyzes the oscillator strength related contributions, visualized as a two-dimensional map. In the map, the x-axis shows the eigenvalues of the occupied Kohn-Sham states, and the y-axis shows those of the unoccupied Kohn-Sham states to which the contributions are decomposed. The red contour plot shows the contributions to the total absorption from the individual electron-hole transitions at the fixed energy matching the analyzed peak. Here, we combine the TCM analysis with atom resolved projected density of states (PDOS). Electron states were projected to the atom orbitals centered at each atom and the data was then collected to analyze the localization of the states. In the TCM figures, the lower-left panel shows the

PDOS of the occupied states and the right panel shows the PDOS of the unoccupied/virtual states. The bottom-right panel shows the absorption spectrum, with the arrow indicating the analyzed peak. The dashed line with the contours represents the excitations exactly at the analyzed energy.

Absorption spectra can be further analyzed with TD-DFPT by calculating the induced density for a specific spectral feature of interest. Here, we calculated the induced transition density of the first absorption peak of the Au_{25}–Mg assembly and its isolated cluster. It is visualized as a contour plot, providing insight into the spatial distribution of the density oscillations.

Additionally, we perform rotational transition contribution map (RTCM) analysis on Au_{25}-Mg to study the CD spectrum. With RTCM, it is possible to determine which parts of the structure contribute to the excitations responsible for chiral activity. RTCM analysis is not performed on the other systems, as it is not implemented for spin-polarized systems in GPAW.

All the calculations were performed in the Finnish CSC - IT Center for Science using Mahti supercomputer. Calculating the ground state for the four cluster assembly required a considerable amount of computational resources. For example, Au_{25}-Mg assembly has 1193 atoms, 4832 valence electrons, and 2756 bands to converge in order to perform LR-TDDFT.

References

[1] S. Kim, H. Jääskö, K. C. Park, S. Malola, H. Häkkinen and S. S. Park, *J. Am. Chem. Soc.*, 2025, **147**, 30803–30808.

[2] C. F. Macrae, I. Sovago, S. J. Cottrell, P. T. A. Galek, P. McCabe, E. Pidcock, M. Platings, G. P. Shields, J. S. Stevens, M. Towler and P. A. Wood, *J. Appl. Crystallogr.*, 2020, **53**, 226–235.

[3] C.-S. Liu, J.-J. Wang, L.-F. Yan, Z. Chang, X.-H. Bu, E. C. Sañudo and J. Ribas, *Inorg. Chem.*, 2007, **46**, 6299–6310.

[4] Y. Liu, W.-J. Shi, Y.-K. Lu, G. Liu, L. Hou and Y.-Y. Wang, *Inorg. Chem.*, 2019, **58**, 16743–16751.

[5] J. J. Mortensen, A. H. Larsen, M. Kuisma, A. V. Ivanov, A. Taghizadeh, A. Peterson, A. Haldar, A. O. Dohn, C. Schäfer, E. Ö. Jónsson, E. D. Hermes, F. A. Nilsson, G. Kastlunger, G. Levi, H. Jónsson, H. Häkkinen, J. Fojt,

J. Kangsabanik, J. Sødequist, J. Lehtomäki, J. Heske, J. Enkovaara, K. T. Winther, M. Dulak, M. M. Melander, M. Ovesen, M. Louhivuori, M. Walter, M. Gjerding, O. Lopez-Acevedo, P. Erhart, R. Warmbier, R. Würdemann, S. Kaappa, S. Latini, T. M. Boland, T. Bligaard, T. Skovhus, T. Susi, T. Maxson, T. Rossi, X. Chen, Y. L. A. Schmerwitz, J. Schiøtz, T. Olsen, K. W. Jacobsen and K. S. Thygesen, *J. Chem. Phys.*, 2024, **160**, 092503.

[6] M. Kuisma, J. Ojanen, J. Enkovaara and T. T. Rantala, *Phys. Rev. B*, 2010, **82**, 115106.

[7] J. P. Perdew, K. Burke and M. Ernzerhof, *Phys. Rev. Lett.*, 1996, **77**, 3865–3868.

[8] W. Humphrey, A. Dalke and K. Schulten, *J. Mol. Graphics*, 1996, **14**, 33–38.

[9] S. Malola, L. Lehtovaara, J. Enkovaara and H. Häkkinen, *ACS Nano*, 2013, **7**, 10263–10270.

[10] X. Andrade, S. Botti, M. A. L. Marques and A. Rubio, *J. Chem. Phys*, 2007, **126**, 184106.

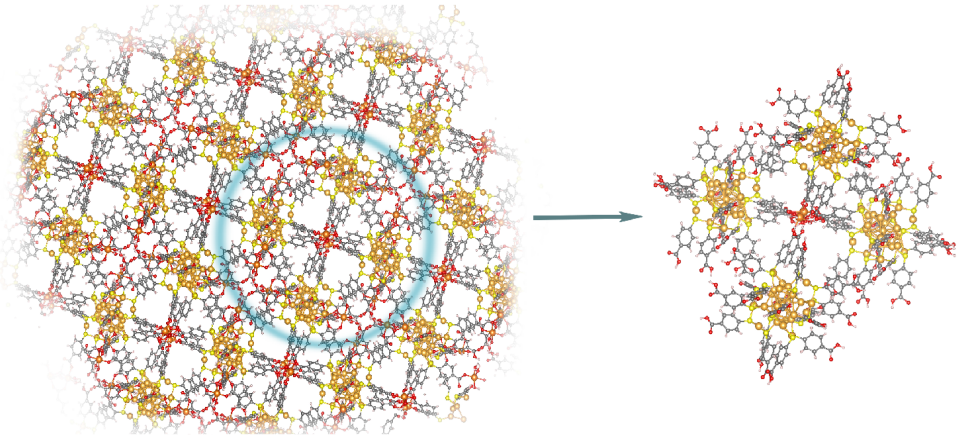

Figure S1. Experimentally determined crystal structure (left), highlighting a region where four Au_{25} clusters are connected through metal ion(s) that form coordination bonds with the carboxylic acid groups. The extracted structure corresponding to that region is shown on the right.

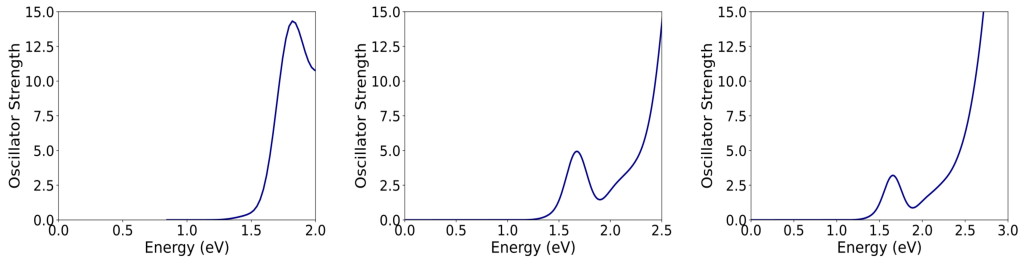

Figure S2. Calculated absorption spectrum for Au_{25}-Mg with different energy cut-offs: 2 eV, 2.5 eV and 3 eV from left to right. No significant differences between the positions of the first peak with 2.5 eV or 3 eV cut-offs.

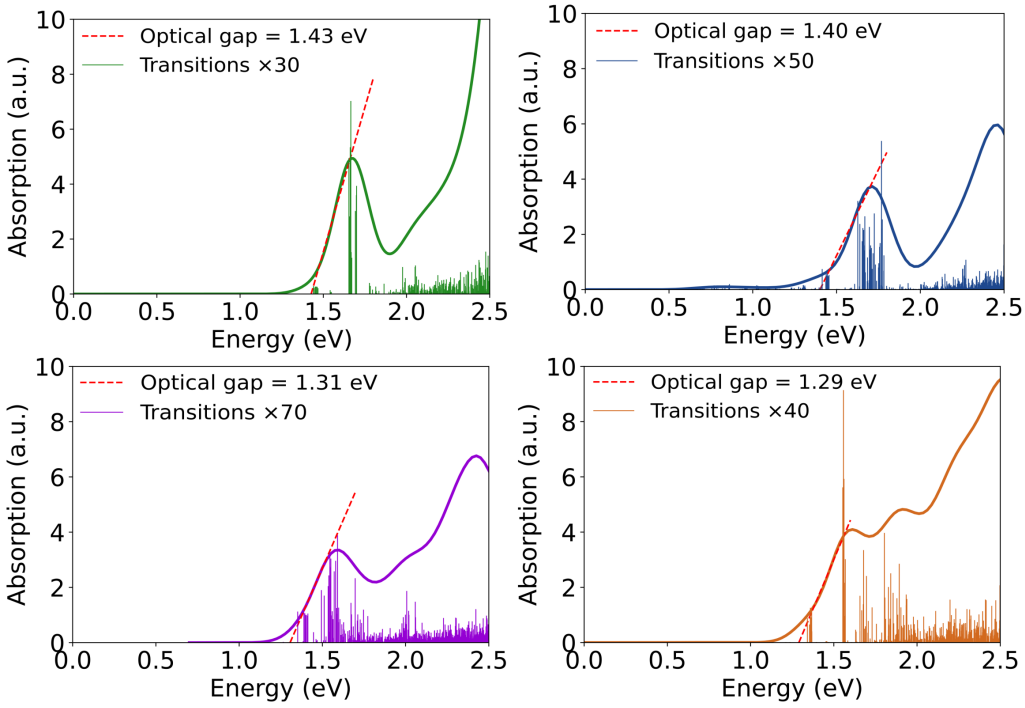

Figure S3. Absorption spectra and oscillator strengths of Au_{25}-Mg, Au_{25}-Co, Au_{25}-Ni and Au_{25}-Cu along with their optical band gaps determined using linear interpolation.

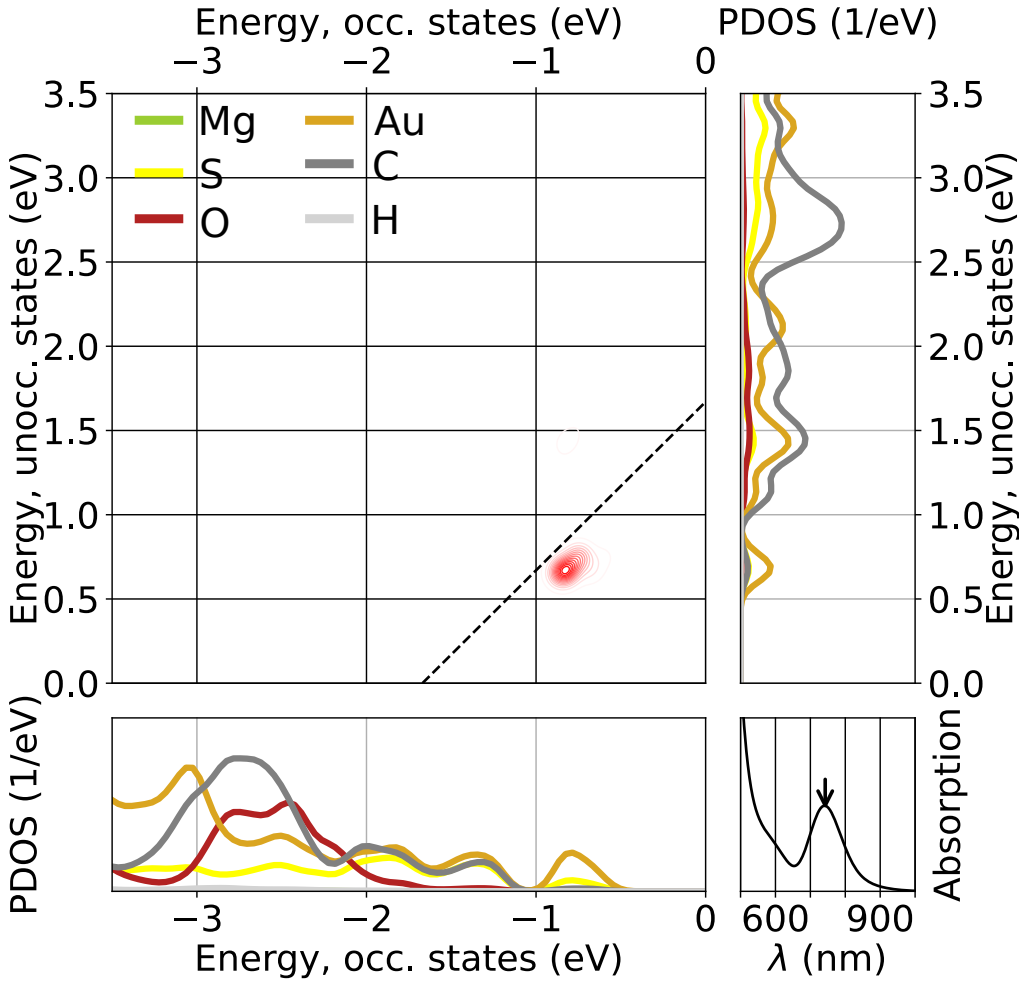

Figure S4. Transition contribution map (TCM) analysis of the first absorption peak of Au_{25}-Mg assembly.

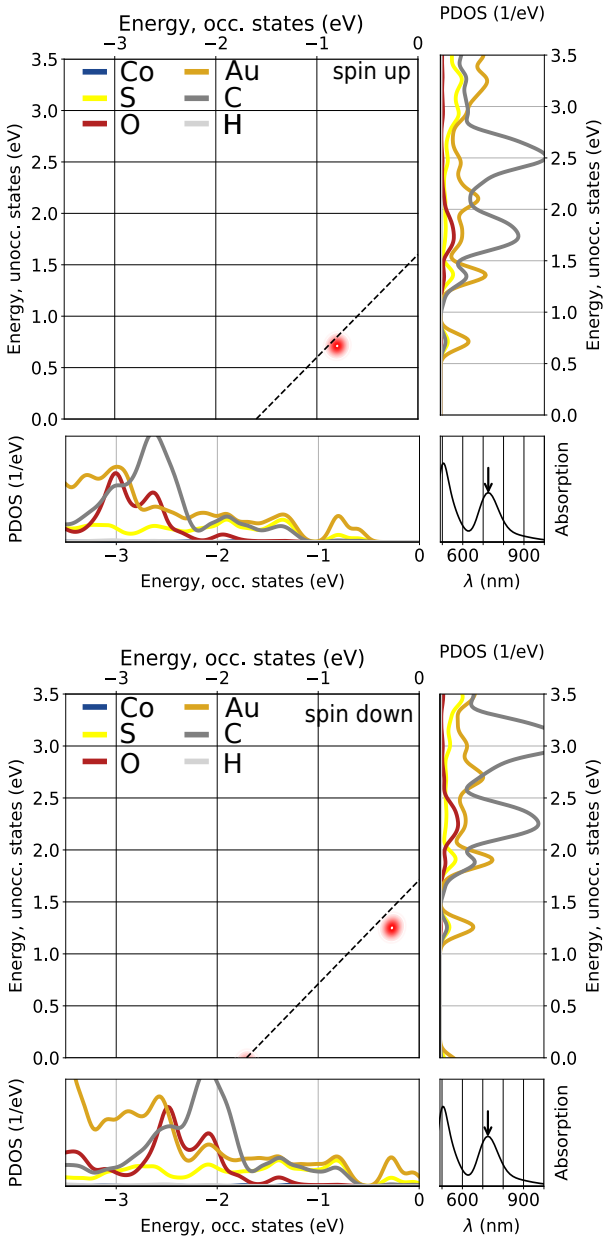

Figure S5. Transition contribution map (TCM) analysis of the first absorption peak of Au_{25}-Co assembly for spin up and spin down contributions.

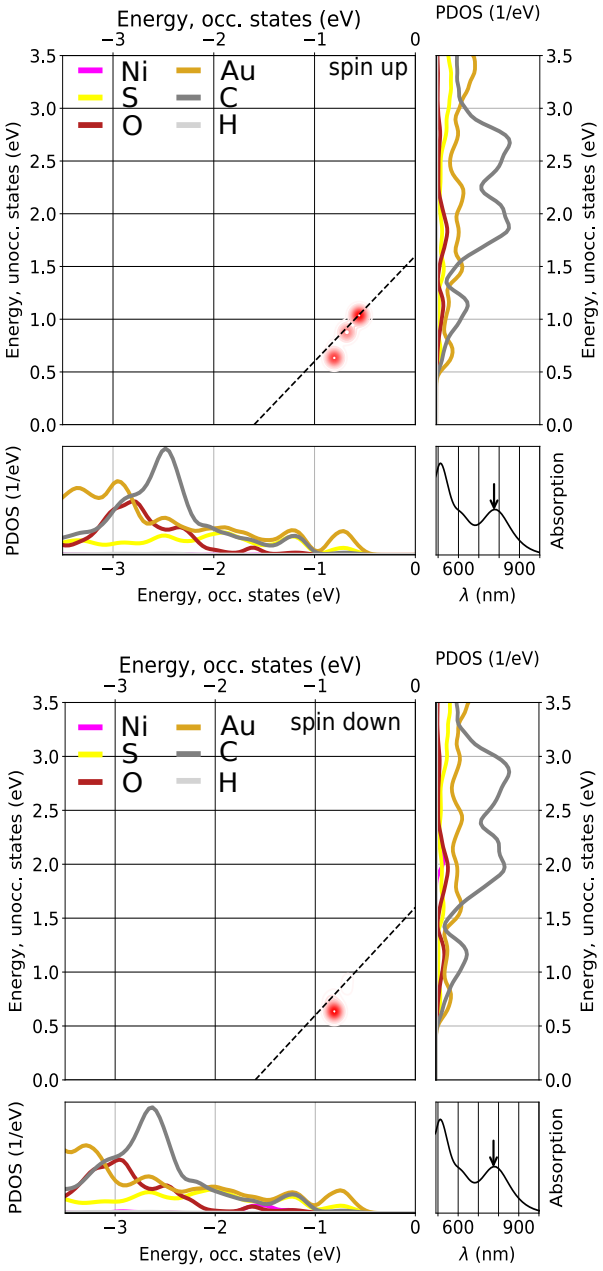

Figure S6. Transition contribution map (TCM) analysis of the first absorption peak of Au_{25}-Ni assembly for spin up and spin down contributions.

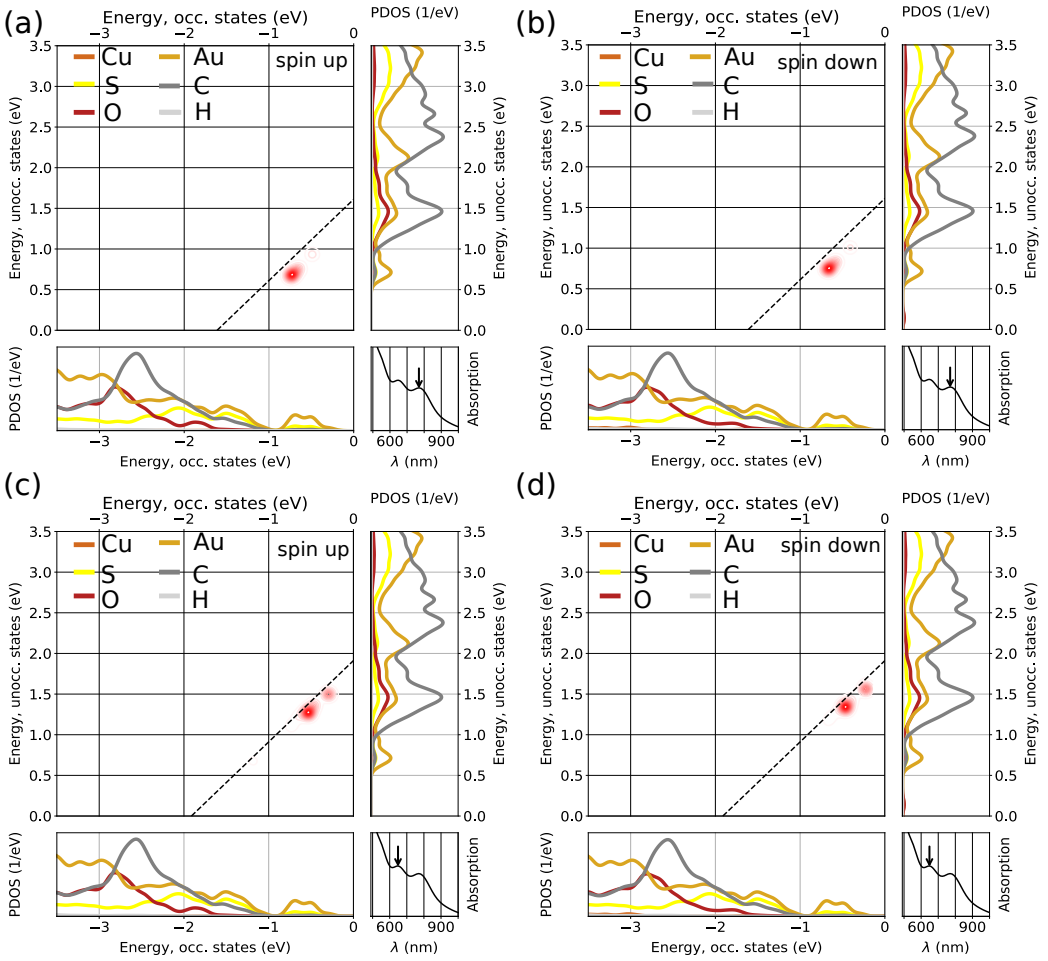

Figure S7. Transition contribution map (TCM) analysis of the first (a), (b) and second (c), (d) absorption peak of Au_{25}-Cu. Transitions for spin up and down are plotted separately.

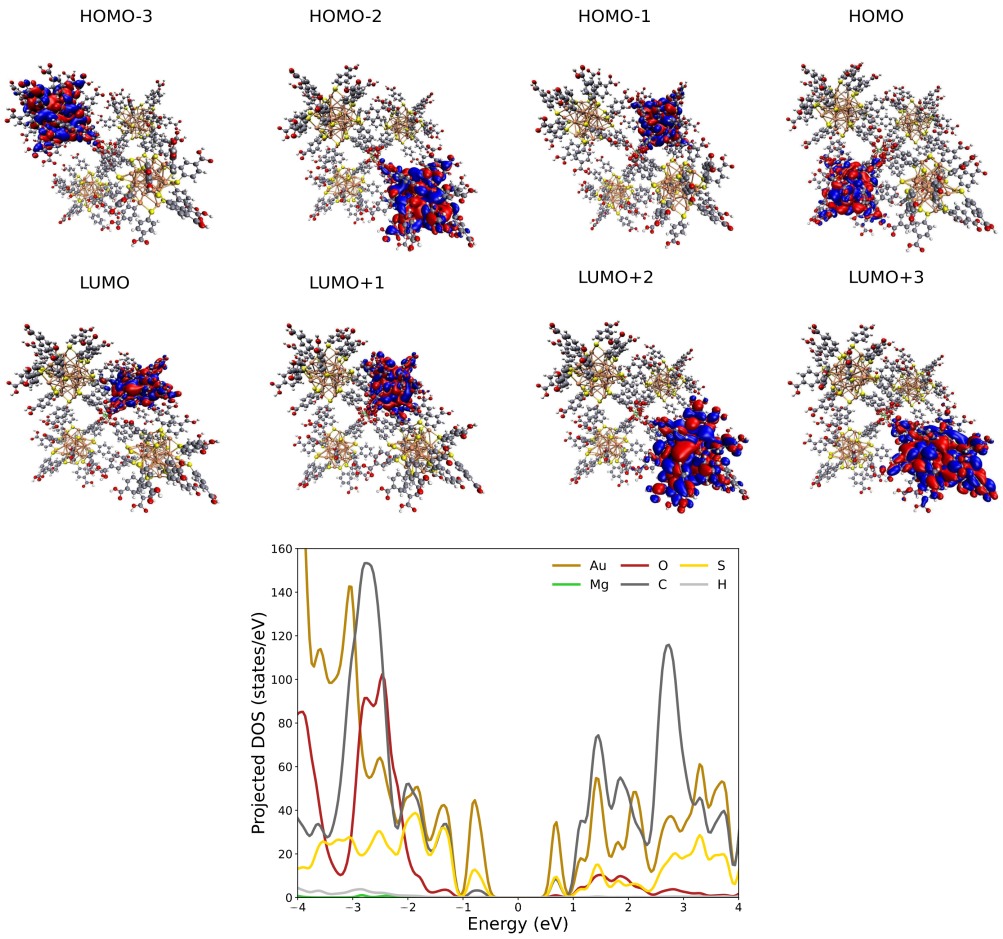

Figure S8. Atom resolved projected density of states (PDOS) and frontier Kohn-Sham orbitals of Au_{25}-Mg assembly.

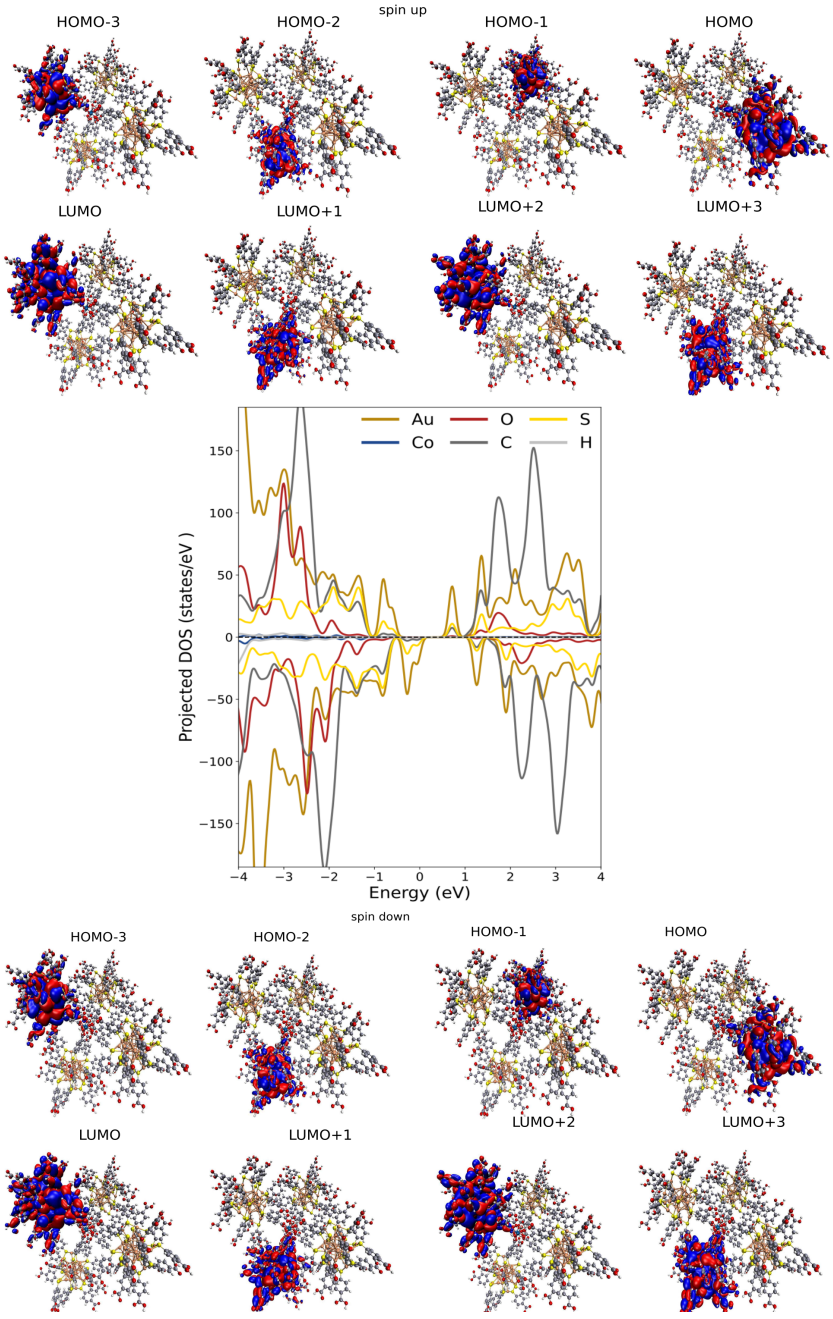

Figure S9. Atom resolved projected density of states (PDOS) and frontier Kohn-Sham orbitals of Au_{25}-Co assembly. Spin up and down are visualized separately.

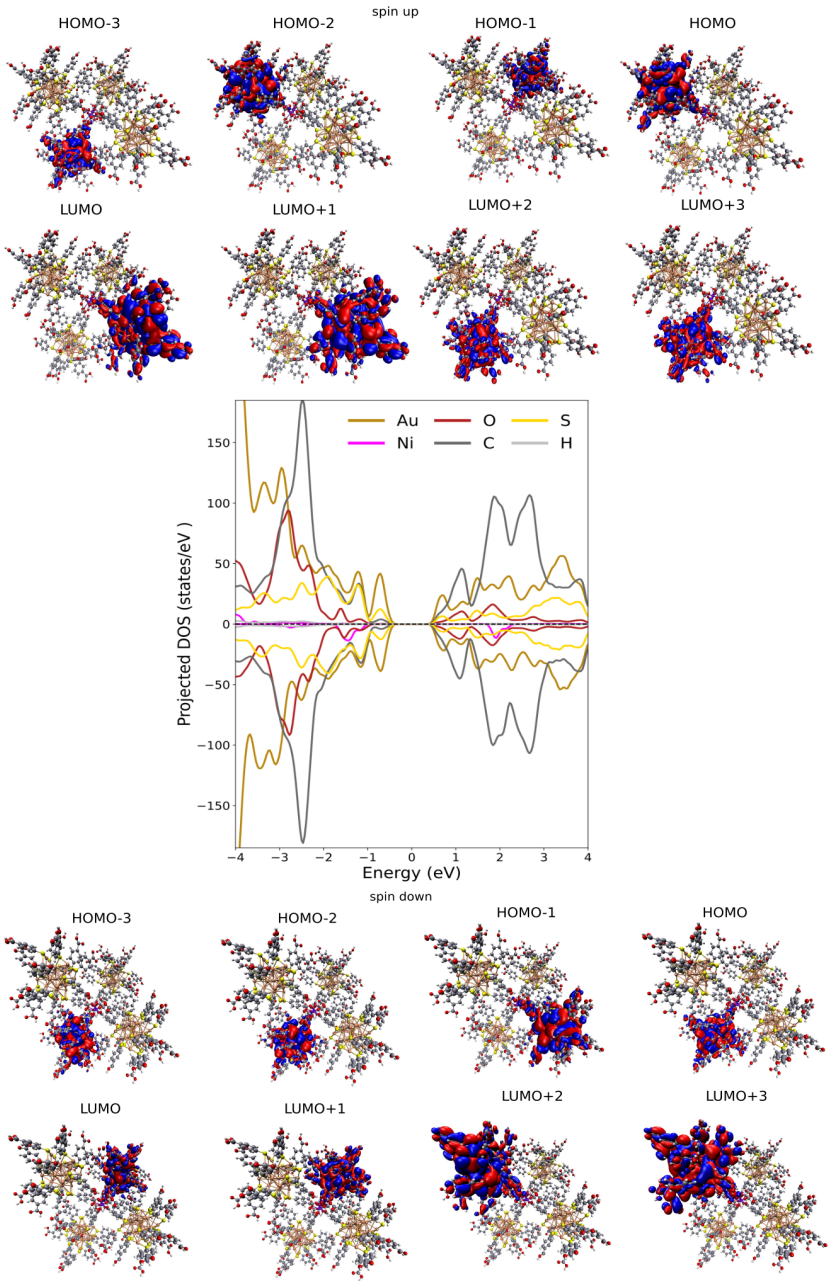

Figure S10. Atom resolved projected density of states (PDOS) and frontier Kohn-Sham orbitals of Au_{25}-Ni assembly. Spin up and down are visualized separately.

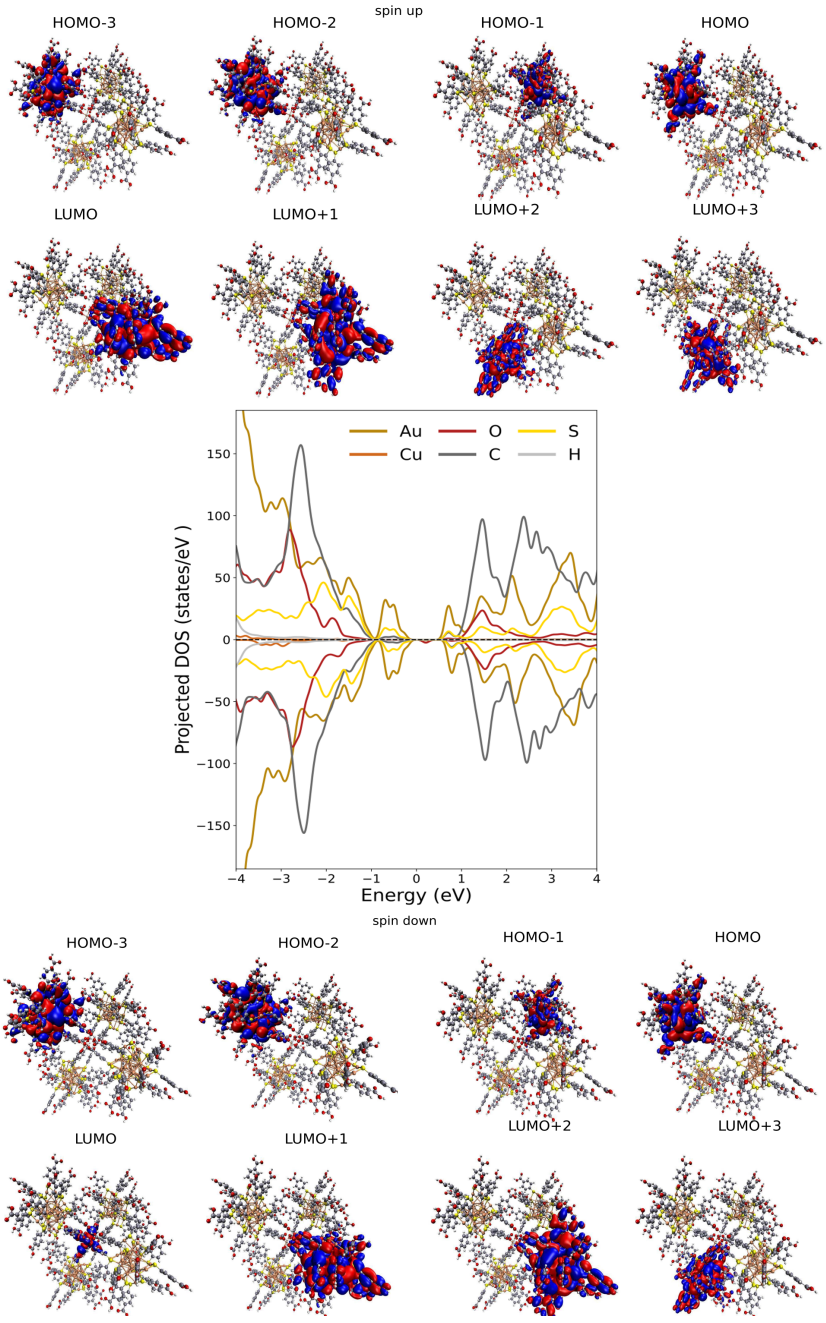

Figure S11. Atom resolved projected density of states (PDOS) and frontier Kohn-Sham orbitals of Au_{25}-Cu assembly.

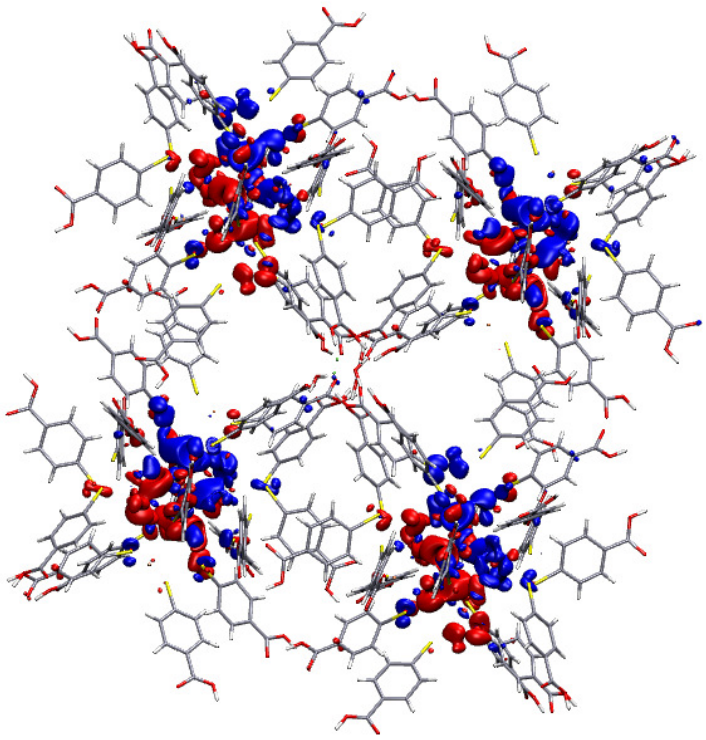

Figure S12. Induced transition density of the first absorption peak of Au_{25}-Mg assembly. Red and blue isosurfaces represent positive and negative values of the induced electron density, visualized along one of the principal axes.

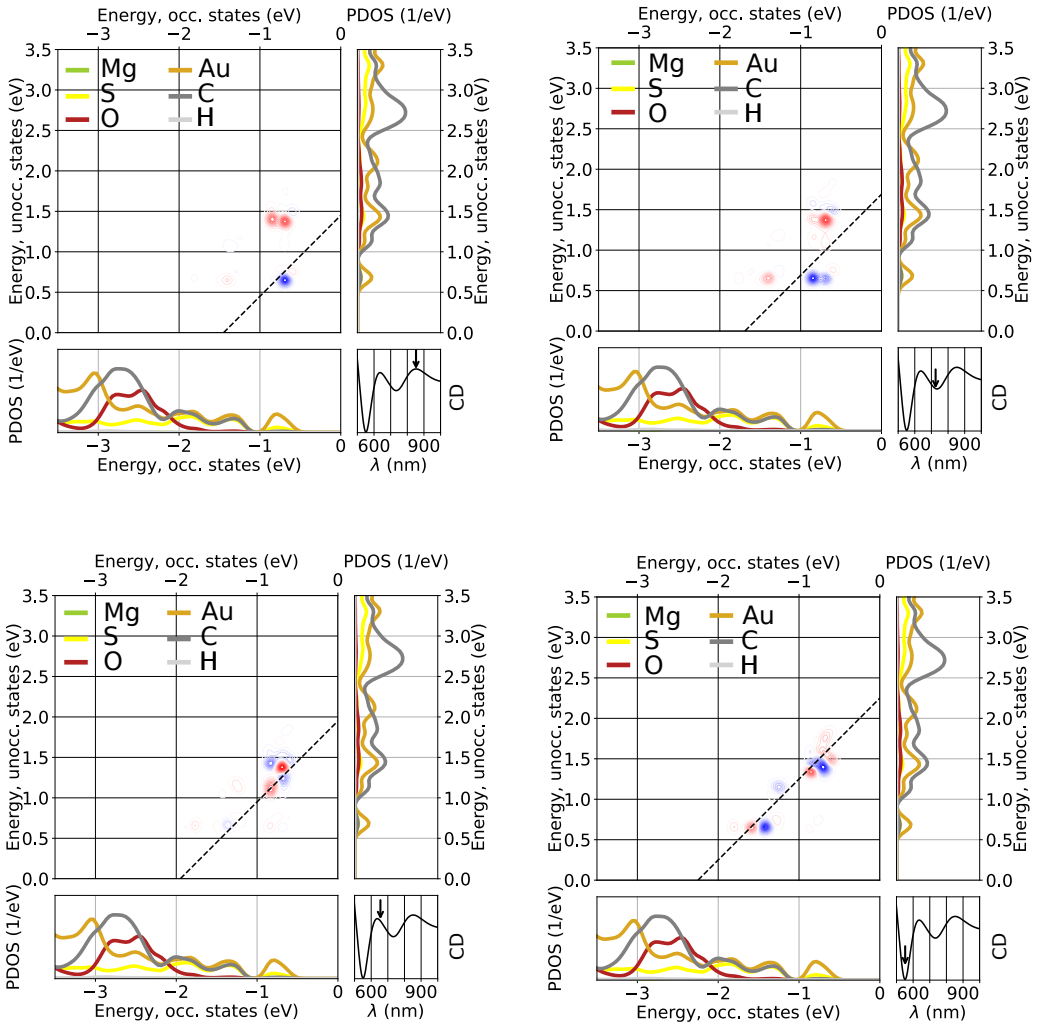

Figure S13. Rotational transition contribution map (RTCM) analysis of Au_{25}-Mg assembly's CD signals. The bottom panel shows the occupied density of states, the right panel shows the unoccupied density of states, and the middle panel shows the rotatory strength transition contributions, with red indicating positive contributions and blue negative contributions. In the bottom-right corner is the CD spectrum and the analyzed peak is marked with an arrow.

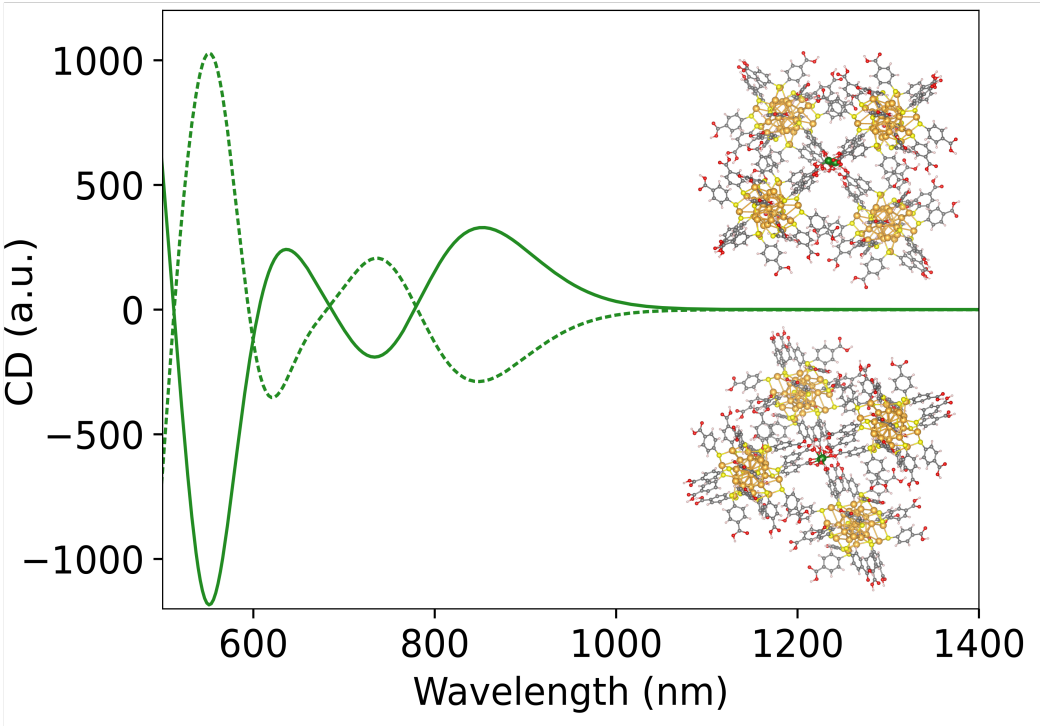

Figure S14. Circular dichroism (CD) spectra of both enantiomers of the Au_{25}-Mg cluster assembly.

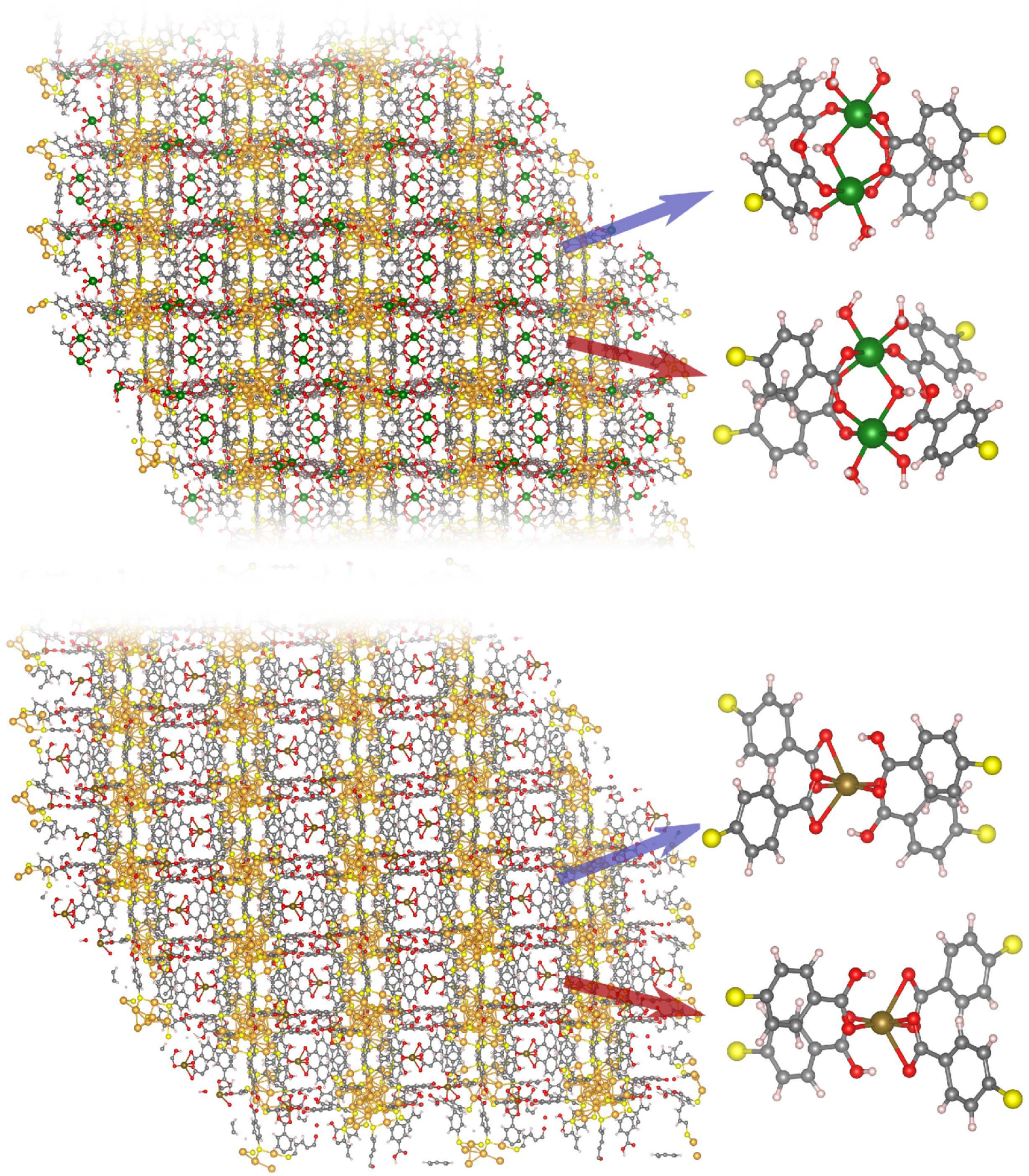

Figure S15. Crystal structures of Au_{25}-Mg (up) and Au_{25}-Cu (bottom) visualized so that the different layers of enantiomers can be seen.